PRELIMINARY STUDY OF THE EFFECT OF OZONE ON ATMOSPHERIC TRANSMISSION IN THE RANGE 0.25 MICRON TO 0.60 MICRON,

MASSACHUSETTS INST OF TECH LEXINGTON

19 FEB 1963

Table of Contents

ABSTRACT

The Project PRESS airborne optical program employs instrumentation having a spectral coverage from 0.25 micron to 15 microns. In relation to PRESS optical measurements, computation of atmospheric transmission in the range 0.25 to 0.60 micron were performed to find the effects of the presence of atmospheric ozone. Graphical and tabular presentations of the transmission through a selected vertical distribution of ozone, which is representative of low latitudes, are given for various target-to-aircraft horizontal distances and for numerous look-angles. The transmission versus wavelength curves show the known atmospheric opaqueness to ultraviolet radiation in the range 0.25 to 0.29 micron. The transmission versus look-angle curves show that maximum absorption, for the particular vertical distribution of ozone used, is experienced between look-angles of eight to ten degrees. This infers that maximum absorption will take place when the PRESS optical instrumentation is recording re-entry phenomena between the heights of 200,000 and 100,000 feet and at a horizontal distance of 80 nautical miles perpendicular to the trajectory. Because of the lack of information about the vertical distribution of ozone at low latitudes, it is recommended that actual measurements be made in the vicinity of Kwajalein prior to the PRESS experiments.

Introduction:

Certain instruments in the Project PRESS airborne optical systems cover the spectral range from 0.25 micron to 0.60 micron. It is necessary to investigate the effects of the intervening atmosphere between the aircraft and the target on the transmission of radiation in the above-mentioned spectral range. Radiation originating at the target can be scattered and absorbed by the air and by such trace substances as dust, ozone and water vapor. In the present report the absorption caused by the presence of ozone is considered alone. Later reports will deal with the effects of scattering and of absorption by other substances.

Procedure:

The depletion of energy caused by the presence of an absorber in a concentration of n molecules per cubic centimeter and with an absorption cross-section σ (cm^2) is given by the relation

$$dI = -I \sigma n \, dx$$

where dI is the energy absorbed in a path length dx. The equation is applicable to monochromatic radiation. Integration of this equation gives:

$$\int_0^x \frac{dI}{I} = -\int_0^x \sigma n \, dx$$

$$I_{(\lambda)} = I_{o(\lambda)} \, e^{-\int_0^x \sigma n \, dx}$$

The transmission of the atmosphere at this particular frequency is thus:

$$\frac{I_\lambda}{I_{o\lambda}} = e^{-\int_0^x \sigma n \, dx} \qquad (1)$$

For a first approximation of the values of the transmission, calculations were performed for a set of path lengths determined by assuming a constant aircraft height of 10.65 km. (35,000 ft), a constant target

to aircraft horizontal distance of 148.5 km (80 nautical miles), and various elevation angles. The paths are shown in Figure 1. In actuality, when Project PRESS is in operation, the slant range and height of the target will be known as a function of time and elevation angle of the optical apparatus from the coordinates of the target and the aircraft. In these preliminary calculations, the curved earth geometry was not used; however it will be used in future calculations of transmission.

To evaluate equation (1), it is necessary to know σ for the particular wavelength of interest and also the concentration n of ozone molecules as a function of height. Now $\sigma = \frac{k}{n_o}$ where n_o is the number of molecules per cubic centimeter at standard temperature and pressure, and k is the Naperian absorption coefficient. These absorption coefficients for ozone as a function of wavelength were taken from the table in the Smithsonian Meteorological Tables, Sixth Edition[1] (actually listed as Decimal absorption coefficients but converted for our purposes to Naperian absorption coefficients). No corrections were made for the possible difference between standard temperature and actual temperatures. The variation of absorption coefficients with temperature is a topic that has not been treated thoroughly from the experimental standpoint up to the present. It is to be noted that there is presently available another set of absorption coefficients (see Paetzold[4]) which differ by approximately 15 to 20 percent from the values selected.

Some ozone soundings are given in units of ozone reduced to standard temperature and pressure in which case the intermediate step of calculating the cross-section need not be used. But for consistency, we have adopted the values of σ as calculated above and expressed the ozone measurements in terms of molecules per cubic centimeter at altitude; it would be expected that ozone measurements reported in the field (e.g. at Kwajalein) would be in these units. The absorption cross-sections as a function of wavelength are listed in Table I.

The major problem in this work was the choice of a distribution of ozone with height appropriate to the Marshall Island region. Total amounts of ozone in a vertical column have been measured for many years (since about 1929) by the Dobson Spectrophotometer (see Mitra[2]). In the Pacific the only measurements of total ozone amounts available

are those at Hawaii (Latitude 21°N) taken since 1959. At latitudes within 10° of the equator the only measurements anywhere in the world are those taken in India (Latitude 10°N) and Leopoldville, Congo (Latitude 4°S). In general the total amount of ozone varies with latitude, has a maximum in middle and high latitudes in the spring, and has the smallest variation with latitude in the fall. There are large variations with longitude in the middle and high latitudes. The day-to-day variability is largest in the middle and high latitudes throughout the year. The variation in the average amount of total ozone at the low latitude Indian station was about 15 percent during the course of the I.G.Y. (1957-1958); during the I.G.C. (1959) the variation was about 20 percent. Figure 2 shows the monthly variation of the average total amount of ozone during the years 1957, 1958, and 1959 for two low latitude stations, Leopoldville Congo (4°S) and Kodai Kanal, India (10°N). The total amount also varies during the course of the sunspot cycle.

Of much more importance from our point of view is the vertical distribution of ozone. This can be obtained indirectly by the so-called "Umkehr" effect using the Dobson instrument[2]. The disadvantage of this technique is that it integrates over deep layers of the atmosphere (usually depths of 6 km. are adopted in the computations). A few profiles taken by this technique are available for India[3] and Leopoldville[4]. These represent the only low latitude data available by this technique. The profiles obtained for middle and high latitudes are considerably different[3,4,5]. A much more satisfactory procedure from the present point of view is to measure the vertical distribution of ozone. Three instruments are available for this measurement; all have attained altitudes of 30 km. They are (a) the Brewer chemical sonde[6], (b) the Paetzold optical sonde[7] and (c) the Regener photoluminiscent device[8]. All have become semi-operational only in the past few years. The only low latitude measurements reported in the literature so far are two Paetzold-sonde profiles[4] taken at Leopoldville (4°S) on October 10, 1958 and November 13, 1958. When actual soundings are compared with Umkehr effect concentrations at middle latitudes (see Paetzold[4]), it is immediately evident that the peak concentrations are grossly underestimated by the Umkehr effect as indeed would be expected. The actual concentrations reported in the November 13, 1958 Leopoldville sounding were used, as this sounding showed the highest

values. For the region below 20 km. where this sounding was not operating, the Umkehr values were selected (Figure 4, Paetzold[7]); for the region above 30 km., values appropriate to Indian Umkehr measurements were selected.[5] The actual composite profile used is shown in Figure 3. No information is available for the region above 60 km., however, in this study it is assumed to be negligible. The values shown were converted to molecular concentrations at altitude. The transmission was calculated as a function of depth in the atmosphere along the six slant paths shown in Figure 1 for the wavelength intervals 0.25 - 0.26 micron, 0.285 - 0.290 micron, 0.300 - 0.301 micron, 0.310 - 0.311 micron, 0.320 - 0.321 micron, 0.330 - 0.331 micron, 0.35 micron, 0.40 micron, 0.45 - 0.46 micron, 0.50-0.51 micron, 0.55 - 0.56 micron and 0.60 - 0.61 micron. No ozone absorption coefficients are available for wavelengths 0.35 to 0.43 micron, therefore it is assumed that no significant ozone absorption takes place at these wavelengths. The above mentioned transmission calculations were done by hand computations. After reviewing the results, a computer program was written so that the transmission could be computed systematically for as many wavelength intervals and look-angles as desired for given horizontal distances away from the re-entry vehicle and for given vertical distributions of ozone.

Results:

The transmission of the atmosphere between the re-entry vehicle altitude and the aircraft for various paths as a function of wavelength is shown in Table II. The atmosphere is essentially opaque to ultraviolet radiation in the range 0.25 to 0.29 micron. For longer wavelengths, the transmission decreases as the vehicle descends reaching a minimum for path 3 and then increases for lower vehicle altitudes. The minimum transmission is directly attributable to the maximum ozone concentration in the layer 20 to 30 km. The experiments will obviously be significantly affected by ozone absorption up to wavelengths of 0.33 micron, and smaller effects will be present for wavelengths 0.45 to 0.60 micron.

Further Computations: While the above approach is satisfactory to establish the presence of significant absorption, it is uneconomical

for use in the general case where it is desired to investigate the effects of the variation of ozone concentrations, target-aircraft distance and look-angle for many wavelengths. For the latter purpose, a computer program was written. With the ozone distribution shown in Figure 3, the transmission has been evaluated (on the IBM 7090) for a series of horizontal target to aircraft distances, ranging from 129.73 km. to 222.39 km. For each horizontal distance, a series of look-angles ranging from 2 degrees to 44 degrees in steps of two degrees were investigated. The results of this more comprehensive study are similar to those of the pilot study, but provide the detail necessary in any engineering consideration. Three representations of the data are given below. In Figure 4, the variation of transmission is given as a function of wavelength for a given horizontal distance of 148.26 km. and for a series of look-angles; 2, 10, 20, and 40 degrees. It should be noted that the transmission is better at 2 and 40 degrees than at 10 degrees. The atmosphere is essentially opaque for wavelengths shorter than 0.30 micron but the exact cut-off depends markedly on the look-angle. A second representation is given in Figure 5 in which the variation of transmission as a function of look-angle is plotted for a series of wavelengths. This brings out rather nicely the strong dependence of the transmission (again for a fixed horizontal distance) on the look-angle. Apart from the minor maximum near 4 degrees which depends on the particular distribution of ozone chosen, there is an increase of transmission with look-angle which starts at about 8 or 10 degrees and presumably continues up to maximum transmission values at vertical incidence. Obviously, if the effect is ignored, it could be concluded that the target was emitting less and less energy as it descended and then suddenly brightening again (at the short wavelengths). As a final presentation of a segment of the results, Figure 6 shows the variation of transmission with look-angle for one wavelength and two different horizontal distances. In the Appendix, some of the actual transmission values as a function of look-angle and wavelength are shown for two horizontal distances (Table I-A and Table II-A).

Ultimately it will be possible to use such calculations to correct the observed fluxes of short wave radiation for the effects of atmospheric

absorption; however, scattering losses will also have to be considered simultaneously. The absorption values are sensitive to the vertical distribution of ozone, and before such corrections can be made, it is imperative to establish the distribution in the vicinity of Kwajalein. Since ozone concentrations vary with latitude, longitude, from month to month and from year to year, it is clearly not satisfactory to make these corrections on the basis of measurements taken several years ago over Africa and India.

Recommendations:

The ozone concentration in the vertical should be measured to 30 km. or higher over the Marshall Islands by one of the three direct sampling techniques mentioned in this paper. If possible the rocket ozone sondes being developed by the Navy at China Lake[9] should also be used to obtain ozone concentrations up to a height of 60 km.

Future Work:

The next step proposed is an examination of the effects of scattering in the same wavelength range (0.25 to 0.60 micron). Scattering will be due to air molecules, dust and water vapor. When this wavelength range has been investigated, it is intended to examine the transmission in the range 0.60 to 16 microns. It is anticipated that the principal absorbers in this range will be carbon dioxide, water vapor and ozone. It is therefore of particular importance to know the vertical distribution of ozone. Outside laboratory help will be called for when the investigation of the longer wavelengths is initiated. Consideration should also be given to the effects on the transmission calculations using curved earth geometry rather than a flat earth as used in the calculation contained in this paper; the effects of different ozone distributions; the effects of different absorption coefficients, since different investigators have listed two sets of absorption coefficients in the literature; and the effects of higher look-angles.

Additional Note:

Since this paper was originally submitted for publication (July 17, 1962) the investigations mentioned in the above paragraph under "Future Work" have been carried out and a comprehensive report describing the results and recommendations is in preparation.

Table I

Absorption Cross Sections as a Function of Wavelength for Ozone

Wavelength $\lambda(\mu)$	Cross Section σ	Wavelength $\lambda(\mu)$	Cross Section σ
(Ultraviolet)			
.250-.260	120.8×10^{-19}	.319-.320	34.28×10^{-21}
.260-.270	104.5×10^{-19}	.320-.321	26.98×10^{-21}
.270-.280	84.9×10^{-19}	.321-.322	22.70×10^{-21}
.280-.285	30.9×10^{-19}	.322-.323	22.29×10^{-21}
.285-.290	22.3×10^{-19}	.323-.324	16.45×10^{-21}
.290-.295	12.8×10^{-19}	.324-.325	16.19×10^{-21}
.295-.300	5.5×10^{-19}	.325-.326	16.04×10^{-21}
.300-.301	3.93×10^{-19}	.326-.327	10.64×10^{-21}
.301-.302	3.45×10^{-19}	.327-.328	11.39×10^{-21}
.302-.303	3.04×10^{-19}	.328-.329	10.20×10^{-21}
.303-.304	2.72×10^{-19}	.329-.330	6.25×10^{-21}
.304-.305	2.44×10^{-19}	.330-.331	7.70×10^{-21}
.305-.306	2.19×10^{-19}	.331-.332	7.82×10^{-21}
.306-.307	1.99×10^{-19}	.332-.333	4.28×10^{-21}
.307-.308	1.72×10^{-19}	.333-.334	5.47×10^{-21}
.308-.309	1.57×10^{-19}	.334-.335	4.47×10^{-21}
.309-.310	1.34×10^{-19}	.335-.336	2.64×10^{-21}
.310-.311	1.15×10^{-19}	.336-.337	3.35×10^{-21}
.311-.312	1.00×10^{-19}	.337-.338	3.42×10^{-21}
.312-.313	88.2×10^{-21}	.338-.339	1.90×10^{-21}
.313-.314	80.39×10^{-21}	.339-.340	2.16×10^{-21}
.314-.315	65.87×10^{-21}	(Visible)	
.315-.316	59.92×10^{-21}	.45-.46	1.71×10^{-22}
.316-.317	49.27×10^{-21}	.50-.51	1.38×10^{-21}
.317-.318	46.71×10^{-21}	.55-.56	3.09×10^{-21}
.318-.319	34.72×10^{-21}	.60-.61	4.21×10^{-21}

Table II

Results of Hand Computations of Atmospheric Transmission

for Six Slant Paths Shown in Figure 1

R.V. Alt. (Km)	Aircraft Alt. (Km)	Slant Range (Km)	Look-Angle (Deg)	Atmospheric Transmission ($\frac{I}{I_o}$) (percent) at Aircraft Level for Specified Wavelengths Using the Vertical Distribution of Ozone in Figure 3										
				λ .25-.26 μ	λ .285-.290 μ	λ .300-.301 μ	λ .310-.311 μ	λ .320-.321μ	λ .330-.331 μ	λ .35-.40 μ	λ .45-.46 μ	λ .50-.51 μ	λ .55-.56 μ	λ .60-.61μ
100	10.65	173.0 (6)	31.2	Opaque	Opaque	0.39	19.8	68.3	89.7	Assume 100% Transmission	99.8	98.1	95.7	94.2
80	10.65	164.5 (5)	25.0	Opaque	Opaque	0.12	15.4	62.9	87.6		99.7	97.7	94.8	93.0
60	10.65	157.5 (4)	18.3	Opaque	Opaque	0.01	6.98	53.5	83.7		99.6	96.9	93.1	90.7
40	10.65	151.5 (3)	11.2	Opaque	Opaque	$\sim 10^{-5}$	1.51	37.4	75.5		99.4	95.1	89.4	85.8
30	10.65	149.5 (2)	7.4	Opaque	Opaque	$\sim 10^{-4}$	2.96	43.6	79.0		99.5	95.8	91.0	87.9
20	10.65	149.0 (1)	3.6	Opaque	$\sim 10^{-5}$	6.66	45.3	83.0	94.8		99.9	99.1	97.9	97.1

NOTES: 1. Path Number in Parenthesis after Slant Range

2. Transmission Values Less Than 10^{-10} are Listed as Opaque.

APPENDIX

Table I-A

Percent Transmission

Wavelength (micron)	2°	4°	6°	8°	10°	12°	14°	16°	18°	20°
.250-.260	0.0000	0.0000	0.0000	0.0000	0.0000	0.0000	0.0000	0.0000	0.0000	0.0000
.280-.285	0.0000	0.0000	0.0000	0.0000	0.0000	0.0000	0.0000	0.0000	0.0000	0.0000
.285-.290	0.0000	0.0000	0.0000	0.0000	0.0000	0.0000	0.0000	0.0000	0.0000	0.0000
.290-.295	0.0002	0.0109	0.0000	0.0000	0.0000	0.0000	0.0000	0.0000	0.0000	0.0000
.295-.300	0.3416	1.989	0.0733	0.0000	0.0000	0.0000	0.0000	0.0000	0.0002	0.0006
.300-.301	1.728	6.085	0.5758	0.0003	0.0000	0.0001	0.0006	0.0027	0.0073	0.0192
.302-.303	4.332	11.47	1.851	0.0049	0.0008	0.0028	0.0093	0.0293	0.0632	0.1332
.304-.305	8.050	17.59	4.068	0.0351	0.0083	0.0223	0.0579	0.1459	0.2740	0.4922
.306-.307	12.81	24.23	7.343	0.1523	0.0472	0.1051	0.2289	0.4864	0.8047	1.311
.308-.309	19.77	32.68	12.74	0.5987	0.2376	0.4469	0.8259	1.497	2.227	3.273
.310-.311	30.50	44.08	22.11	2.354	1.196	1.900	2.980	4.606	6.162	8.171
.314-.315	50.[illegible]	62.55	42.13	11.68	7.925	10.33	13.37	17.15	20.27	23.82
.318-.319	69.87	78.09	63.41	32.24	26.28	30.22	34.62	39.49	43.11	46.95
.322-.323	79.44	85.32	74.64	48.35	42.41	46.39	50.61	55.07	58.27	61.54
.326-.327	89.60	92.70	86.97	70.69	66.40	69.30	72.25	75.22	77.27	79.32
.330-.331	92.36	94.66	90.39	77.80	74.35	76.69	79.04	81.38	82.98	84.56
.334-.335	95.49	96.87	94.30	86.44	84.19	85.72	87.24	88.72	89.73	90.72
.338-.339	98.06	98.66	97.54	93.99	92.95	93.66	94.36	95.04	95.50	95.95
.339-.340	97.79	98.47	97.21	93.20	92.02	92.83	93.61	94.38	94.90	95.40
.450-.460	99.82	99.88	99.78	99.44	99.34	99.41	99.48	99.54	99.59	99.63
.500-.510	98.59	99.02	98.21	95.60	94.83	95.36	95.87	96.37	96.71	97.04
.550-.560	96.86	97.82	96.03	90.42	88.79	89.90	90.99	92.06	92.79	93.49
.600-.610	95.75	97.05	94.63	87.18	85.04	86.49	87.93	89.34	90.30	91.24

Horizontal Distance = 148.26 km

Aircraft Altitude = 10.668 km

Table I-A (Continued)

Percent Transmission

Wavelength (micron)	22°	24°	26°	28°	30°	32°	34°	36°	38°	40°
.250-.260	0.0000	0.0000	0.0000	0.0000	0.0000	0.0000	0.0000	0.0000	0.0000	0.0000
.280-.285	0.0000	0.0000	0.0000	0.0000	0.0000	0.0000	0.0000	0.0000	0.0000	0.0000
.285-.290	0.0000	0.0000	0.0000	0.0000	0.0000	0.0000	0.0000	0.0000	0.0000	0.0000
.290-.295	0.0000	0.0000	0.0000	0.0000	0.0000	0.0000	0.0000	0.0000	0.0000	0.0000
.295-.300	0.0018	0.0043	0.0087	0.0170	0.0295	0.0467	0.0686	0.0994	0.1356	0.1818
.300-.301	0.0411	0.0758	0.1253	0.2026	0.3004	0.4167	0.5489	0.7151	0.8929	1.101
.302-.303	0.2401	0.3858	0.5690	0.8252	1.119	1.442	1.784	2.189	2.599	3.057
.304-.305	0.7897	1.155	1.578	2.127	2.716	3.329	3.949	4.654	5.342	6.085
.306-.307	1.928	2.630	3.392	4.327	5.282	6.234	7.167	8.195	9.170	10.20
.308-.309	4.437	5.669	6.928	8.395	9.825	11.20	12.50	13.89	15.18	16.51
.310-.311	10.21	12.22	14.15	16.29	18.28	20.12	21.80	23.56	25.14	26.73
.314-.315	27.06	29.99	32.63	35.36	37.78	39.91	41.79	43.69	45.35	46.97
.318-.319	50.21	53.01	55.41	57.82	59.86	61.62	63.14	64.63	65.91	67.14
.322-.323	64.26	66.53	68.45	70.35	71.93	73.28	74.44	75.56	77.52	77.44
.326-.327	80.77	82.32	83.45	84.54	85.45	86.21	86.86	87.48	88.01	88.51
.330-.331	85.83	86.87	87.73	88.56	89.24	89.82	90.31	90.77	91.17	91.55
.334-.335	91.51	92.15	92.68	93.19	93.61	93.96	94.25	94.54	94.77	95.00
.338-.339	96.30	96.59	96.82	97.05	97.23	97.39	97.51	97.64	97.74	97.84
.339-.340	95.80	96.13	96.39	96.65	96.85	97.03	97.18	97.32	97.44	97.55
.450-.460	99.66	99.69	99.71	99.73	99.75	99.76	99.77	99.79	99.79	99.80
.500-.510	97.30	97.51	97.68	97.85	97.98	98.09	98.19	98.28	98.36	98.43
.550-.560	94.05	94.51	94.88	95.24	95.54	95.78	95.99	96.19	96.36	96.52
.600-.610	91.99	92.59	93.09	93.57	93.97	94.30	94.58	94.85	95.07	95.28

Table I-A (Continued)

Percent Transmission

Wavelength (micron)	42°	44°
.250-.260	0.0000	0.0000
.280-.285	0.0000	0.0000
.285-.290	0.0000	0.0000
.290-.295	0.0001	0.0001
.295-.300	0.2326	0.2867
.300-.301	1.313	1.525
.302-.303	3.503	3.932
.304-.305	6.788	7.447
.306-.307	11.15	12.02
.308-.309	17.71	18.80
.310-.311	28.14	29.40
.314-.315	48.37	49.60
.318-.319	68.19	69.10
.322-.323	78.21	78.88
.326-.327	88.93	89.29
.330-.331	91.86	92.13
.334-.335	95.19	95.35
.338-.339	97.93	97.99
.339-.340	97.65	97.73
.450-.460	99.81	99.82
.500-.510	98.49	98.54
.550-.560	96.65	96.76
.600-.610	95.46	95.62

Table II-A

Percent Transmission

Wavelength (micron)	2°	4°	6°	8°	10°	12°	14°	16°	18°	20°
.250-.260	0.0000	0.0000	0.0000	0.0000	0.0000	0.0000	0.0000	0.0000	0.0000	0.0000
.280-.285	0.0000	0.0000	0.0000	0.0000	0.0000	0.0000	0.0000	0.0000	0.0000	0.0000
.285-.290	0.0000	0.0000	0.0000	0.0000	0.0000	0.0000	0.0000	0.0000	0.0000	0.0000
.290-.295	0.0000	0.0008	0.0000	0.0000	0.0000	0.0000	0.0000	0.0000	0.0000	0.0000
.295-.300	0.0925	0.6504	0.0000	0.0000	0.0000	0.0000	0.0000	0.0000	0.0001	0.0006
.300-.301	0.6798	2.738	0.0000	0.0000	0.0000	0.0000	0.0005	0.0026	0.0075	0.0191
.302-.303	2.105	6.184	0.0000	0.0000	0.0002	0.0016	0.0087	0.0289	0.0647	0.1332
.304-.305	4.510	10.71	0.0009	0.0004	0.0031	0.0148	0.0550	0.1447	0.2756	0.4922
.306-.307	7.987	16.17	0.0077	0.0044	0.0213	0.0752	0.2198	0.4831	0.8173	1.311
.308-.309	13.62	23.76	0.0572	0.0367	0.1273	0.3434	0.7999	1.489	2.254	3.274
.310-.311	23.21	34.89	0.4217	0.3048	0.7573	1.567	2.911	4.588	6.217	8.171
.314-.315	43.32	54.71	4.362	3.621	6.099	9.250	13.19	17.12	20.37	23.82
.318-.319	64.34	72.77	19.18	17.39	22.89	28.51	34.38	39.44	43.23	46.95
.322-.323	75.35	81.54	34.65	32.53	38.81	44.68	50.38	55.03	58.37	61.54
.326-.327	87.36	90.72	60.29	58.51	63.65	68.08	72.09	75.19	77.34	79.32
.330-.331	90.68	93.19	69.34	67.85	72.11	75.71	78.91	81.36	83.03	84.56
.334-.335	94.48	95.99	80.85	79.84	82.71	85.08	87.16	88.71	89.77	90.72
.338-.339	97.62	98.28	91.36	90.87	92.25	93.36	94.32	95.04	95.51	95.95
.339-.340	97.29	98.04	90.24	89.69	91.24	92.49	93.57	94.38	94.92	95.40
.450-.460	99.78	99.84	99.19	99.14	99.28	99.38	99.48	99.54	99.59	99.63
.500-.510	98.26	98.74	93.65	93.28	94.31	95.13	95.84	96.37	96.72	97.04
.550-.560	96.15	97.21	86.33	85.58	87.70	89.43	90.93	92.05	92.81	93.49
.600-.610	94.79	96.22	81.86	80.89	83.63	85.89	87.86	89.33	90.33	91.24

Horizontal Distance = 203.85 km

Aircraft Altitude = 10.668 km

Table II-A (Continued)

Percent Transmission

Wavelength (micron)	22°	24°	26°	28°	30°	32°	34°	36°	38°	40°
.250-.260	0.0000	0.0000	0.0000	0.0000	0.0000	0.0000	0.0000	0.0000	0.0000	0.0000
.280-.285	0.0000	0.0000	0.0000	0.0000	0.0000	0.0000	0.0000	0.0000	0.0000	0.0000
.285-.290	0.0000	0.0000	0.0000	0.0000	0.0000	0.0000	0.0000	0.0000	0.0000	0.0000
.290-.295	0.0000	0.0000	0.0000	0.0000	0.0000	0.0000	0.0000	0.0000	0.0000	0.0000
.295-.300	0.0019	0.0045	0.0095	0.0176	0.0295	0.0474	0.0705	0.0985	0.1347	0.1794
.300-.301	0.0436	0.0783	0.1341	0.2083	0.3004	0.4216	0.5598	0.7112	0.8887	1.091
.302-.303	0.2518	0.3959	0.5999	0.8432	1.119	1.455	1.811	2.180	2.590	3.034
.304-.305	0.8203	1.180	1.647	2.164	2.716	3.353	3.998	4.638	5.327	6.049
.306-.307	1.989	2.675	3.512	4.388	5.282	6.271	7.239	8.172	9.148	10.15
.308-.309	4.547	5.745	7.120	8.489	9.826	11.25	12.60	13.86	15.16	16.45
.310-.311	10.39	12.34	14.44	16.42	18.28	20.18	21.93	23.52	25.11	26.65
.314-.315	27.34	30.16	33.00	35.53	37.78	39.99	41.93	43.65	45.31	46.89
.318-.319	50.49	53.16	55.75	57.96	59.86	61.68	63.25	64.60	65.88	67.09
.322-.323	64.48	66.66	68.72	70.46	71.94	73.33	74.52	75.54	76.50	77.39
.326-.327	81.10	82.40	83.60	84.61	85.45	86.24	86.90	87.47	88.00	88.49
.330-.331	85.94	86.93	87.85	88.61	89.24	89.84	90.34	90.76	91.16	91.53
.334-.335	91.58	92.19	92.75	93.22	93.61	93.97	94.27	94.53	94.77	94.99
.338-.339	96.33	96.60	96.85	97.06	97.23	97.39	97.52	97.64	97.74	97.84
.339-.340	95.84	96.15	96.43	96.66	96.86	97.04	97.19	97.32	97.44	97.55
.450-.460	99.66	99.69	99.71	99.73	99.75	99.76	99.77	99.79	99.79	99.80
.500-.510	97.32	97.52	97.70	97.86	97.98	98.10	98.20	98.28	98.36	98.43
.550-.560	94.10	94.53	94.93	95.26	95.54	95.79	96.00	96.19	96.35	96.51
.600-.610	92.05	92.63	93.16	93.60	93.97	94.31	94.60	94.84	95.07	95.27

Table II-A (Continued)

Percent Transmission

Wavelength (micron)	42°	44°
.250-.260	0.0000	0.0000
.280-.285	0.0000	0.0000
.285-.290	0.0000	0.0000
.290-.295	0.0000	0.0001
.295-.300	0.2326	0.2895
.300-.301	1.313	1.535
.302-.303	3.503	3.953
.304-.305	6.788	7.479
.306-.307	11.15	12.07
.308-.309	17.71	18.85
.310-.311	28.14	29.46
.314-.315	48.38	49.66
.318-.319	68.20	69.14
.322-.323	78.21	78.91
.326-.327	88.93	89.31
.330-.331	91.86	92.14
.334-.335	95.19	95.36
.338-.339	97.93	98.00
.339-.340	97.65	97.73
.450-.460	99.81	99.82
.500-.510	98.49	98.54
.550-.560	96.65	96.77
.600-.610	95.46	95.62

List of Figures

References:

1. List, R. J., 1951: Smithsonian Meteorological Tables, 6th Ed., Smithsonian Institution, Washington, D. C., pp 428-429.

2. Mitra, S. K., 1952: The Upper Atmosphere, 2nd Ed., The Asiatic Society, Calcutta, pp 119-162.

3. Ramanathan, K. R. and Kulkarni, R N., 1960: Mean Meridional Distributions of Ozone in Different Seasons Calculated from Umkehr Observations and Probable Vertical Transport Mechanisms: Quart. J. R. Meteor. Soc., 86, pp 144-155.

4. Paetzold, H. K., 1961: Messungen des atmospharischen Ozons: Chapt. 4, Handbuch der Aerologie, Ed. W. Hesse: Akademische Verlagsgesellschaft. Geest and Portig K. - G.; pp 458-531.

5. Mateer, C. L. and Godson, W. L., 1960: The Vertical Distribution of Atmospheric Ozone over Canadian Stations from Umkehr Observations: Quart. J. R. Meteor. Soc., 86, pp 512-517.

6. Brewer, A. W. and Milford, J. R., 1960: The Oxford-Kew Ozone Sonde: Proc. Roy. Soc., 256, pp 470-495.

7. Paetzold, H. K. and Piscalar, F., 1961: Die Messung der vertikalen Ozonverteilung mittels einer optischen Radiosonde: Beitrage zur Physik der Atmosphare, 34, pp 53-68.

8. Regener, V. H., 1960: On a Sensitive Method for the Recording of Atmospheric Ozone: J. Geophy. Res., 65, pp 3975-3977.

9. Krueger, A. J., 1961: Status of the Rocket Ozonesonde Program: Paper Presented at International Ozone Conference, Arosa, Switzerland, 9 August 1961.

DISTRIBUTION

Lincoln Laboratory

Cramer, Felix
Curtis, Harold O.
deRidder, Christa M.
Fuller, Roger L.
Guethlen, Victor J.
Jankowitz, Gerald
Kramer, Robert
Kresa, Kent
Meyer, James H.
Page, Daniel A.
Price, Gary H.

Hawaii

Ellis, Robert H.
Wilkinson, John E.

Kwajalein

Batman, Donald
Benn, Bernard J.
Bressel, Charles N.
Bressel, Ellen R.
Briscoe, Howard W.
Brown, J. Royce
Brown, Robert R.
Curry, George R.
Edelberg, Seymour
Falzone, Charles W.
Flink, Arthur H.
Hubert, Ronald E.
Johnson, Kent R.
Knight, James
Martinson, Robert M.
Michaud, Roland W.
Morriello, Joseph
Ralston, Kenneth E.
Romaine, William R.
Sebring, Paul B.
Shimmin, Herbert S.
Stinnett, Aubrey J.

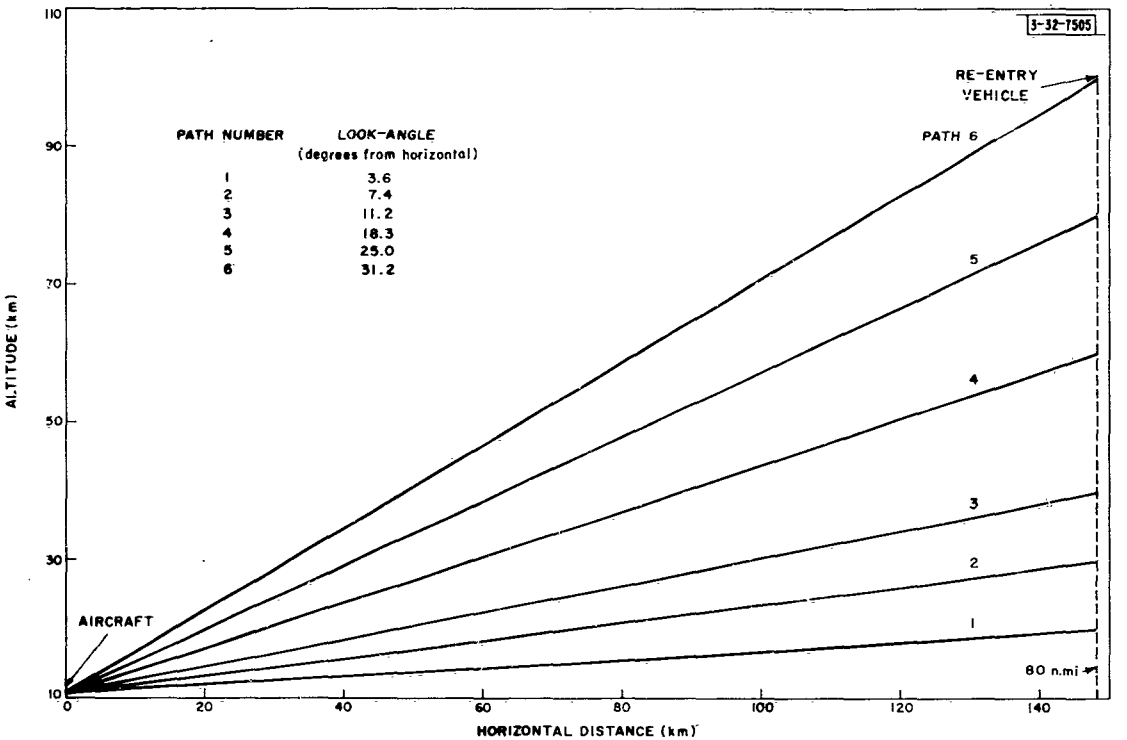
3-32-7505
RE-ENTRY VEHICLE
PATH NUMBER
LOOK-ANGLE (degrees from horizontal)
1 3.6
2 7.4
3 11.2
4 18.3
5 25.0
6 31.2
PATH 6
5
4
3
2
1
AIRCRAFT
80 n.mi
ALTITUDE (km)
HORIZONTAL DISTANCE (km)
110
90
70
50
30
10
0
20
40
60
80
100
120
140

Fig. 1.

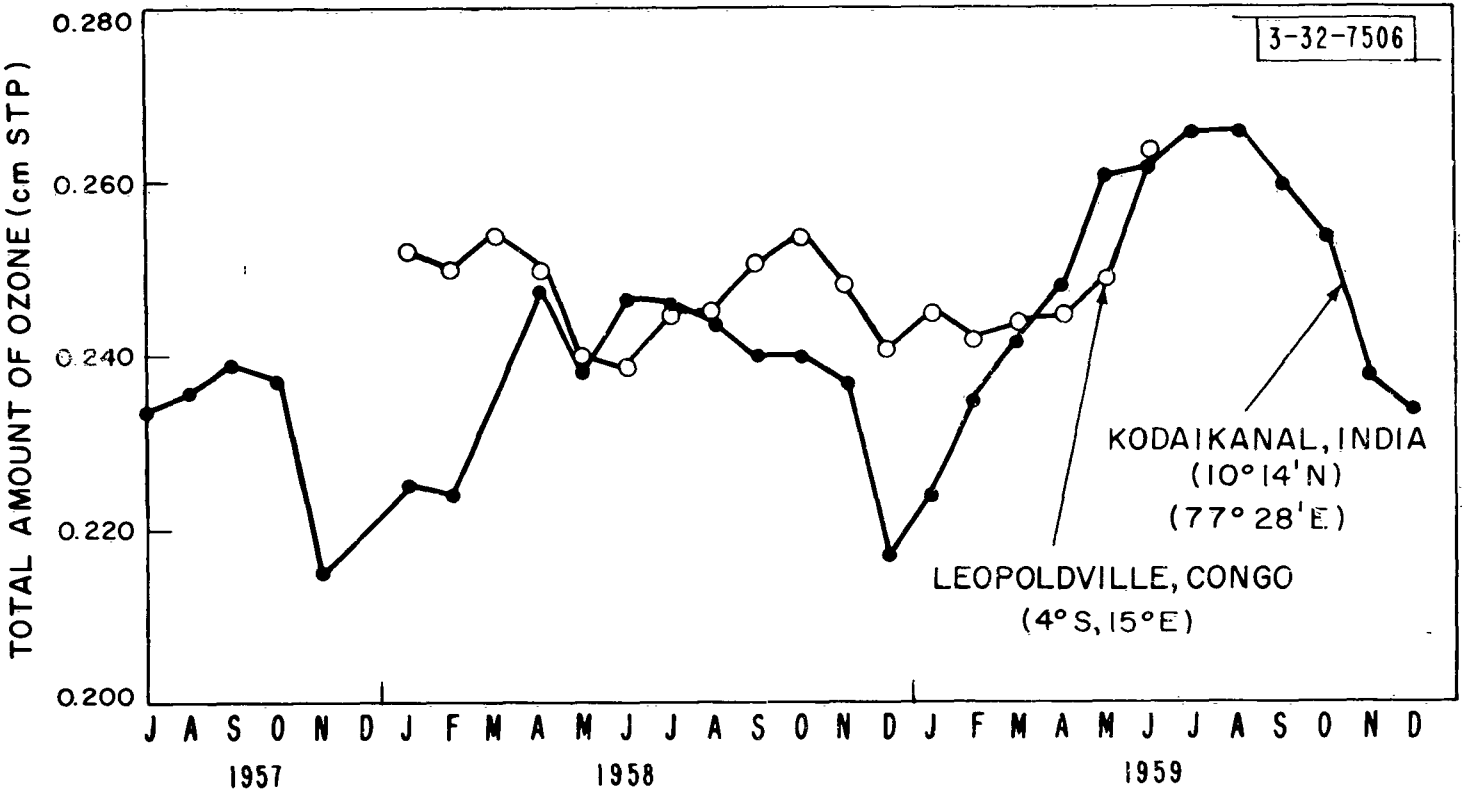
3-32-7506
TOTAL AMOUNT OF OZONE (cm STP)
0.280
0.260
0.240
0.220
0.200
KODAIKANAL, INDIA
(10° 14' N)
(77° 28' E)
LEOPOLDVILLE, CONGO
(4° S, 15° E)
J A S O N D J F M A M J J A S O N D J F M A M J J A S O N D
1957
1958
1959

Fig. 2.

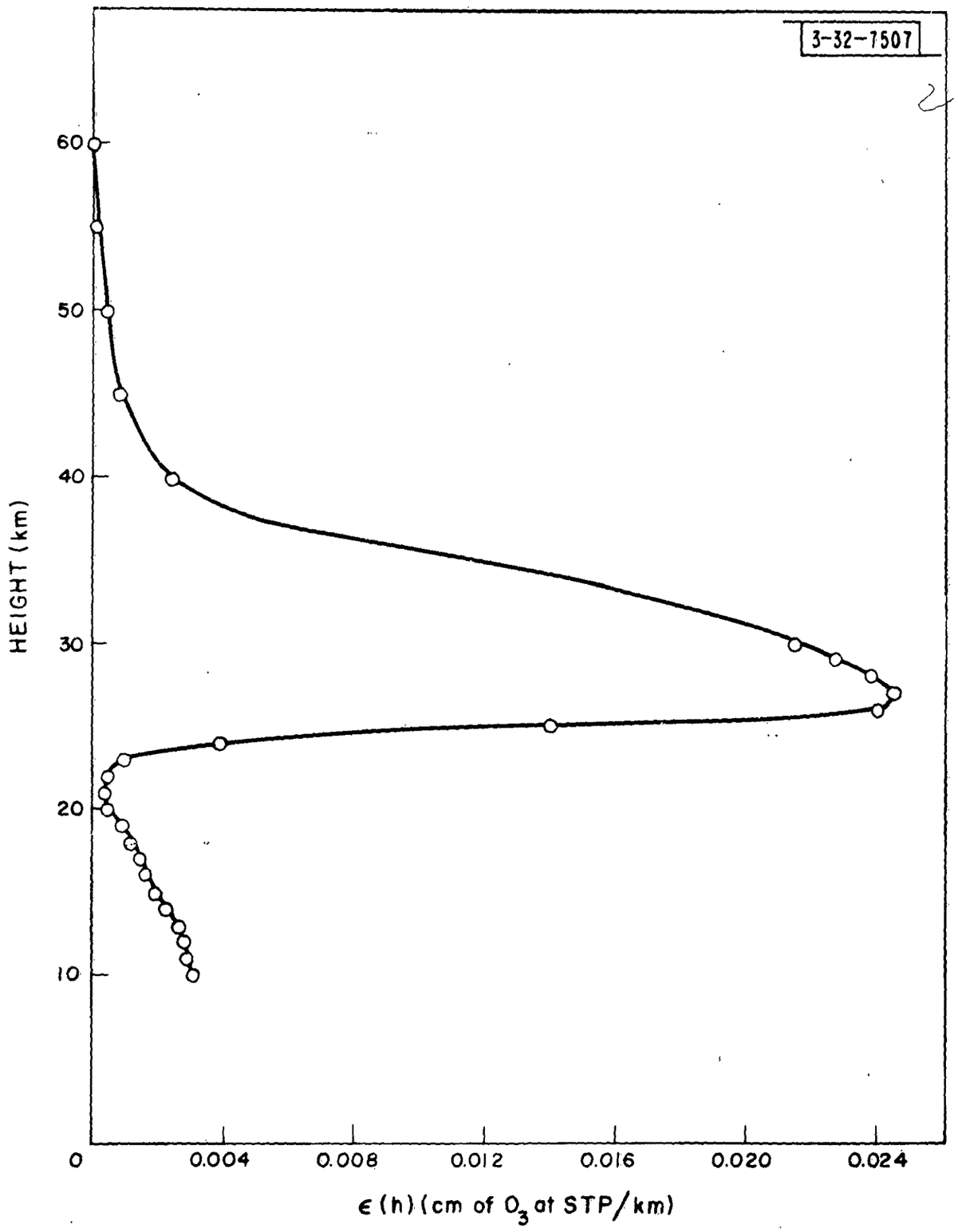
3-32-7507
60
50
40
30
20
10
0
HEIGHT (km)
0.004
0.008
0.012
0.016
0.020
0.024
ε (h) (cm of O3 at STP/km)

Fig. 3.

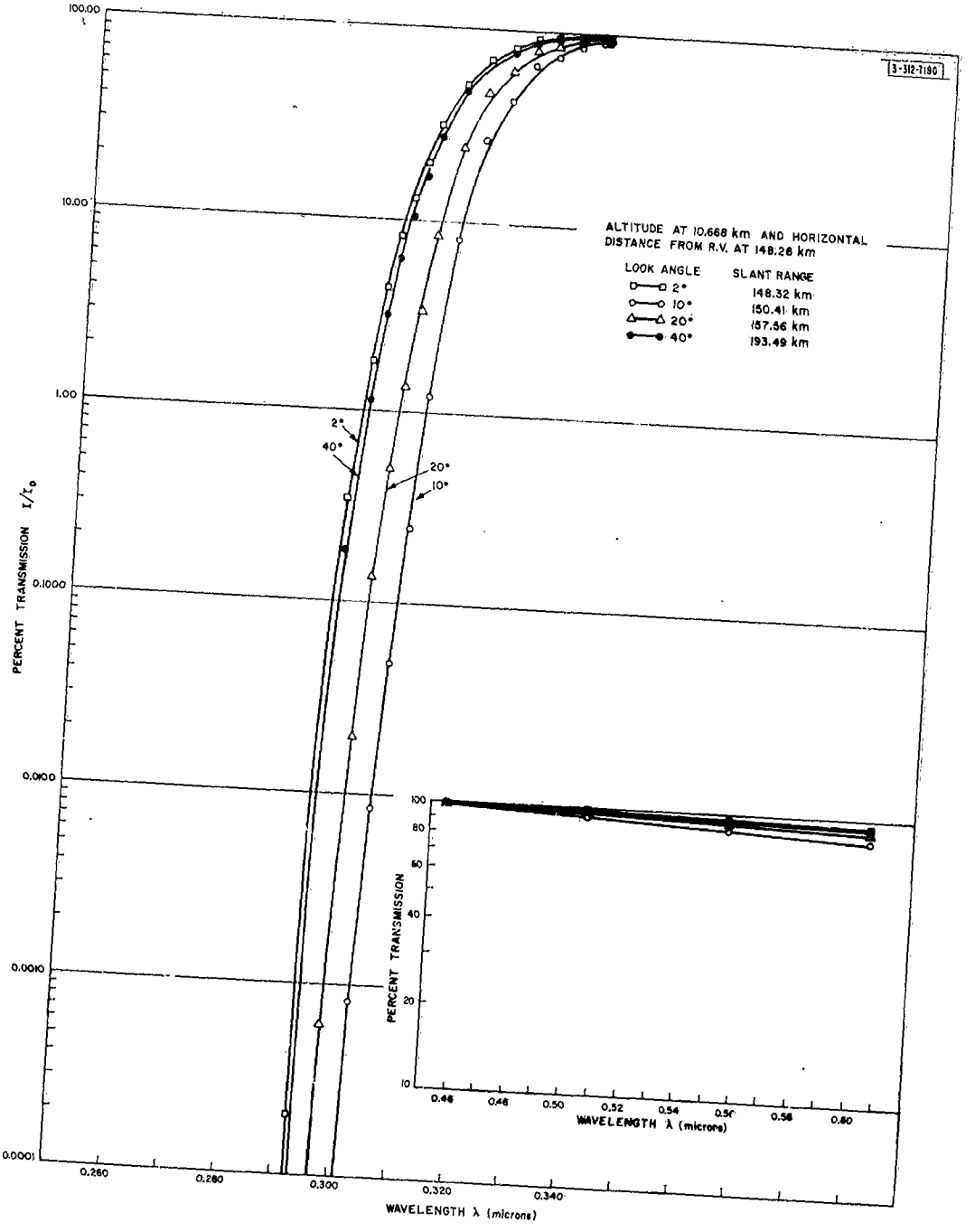
3-312-7190
ALTITUDE AT 10.668 km AND HORIZONTAL DISTANCE FROM R.V. AT 148.28 km
LOOK ANGLE
SLANT RANGE
2° 148.32 km
10° 150.41 km
20° 157.56 km
40° 193.49 km
PERCENT TRANSMISSION I/I0
WAVELENGTH λ (microns)
PERCENT TRANSMISSION
WAVELENGTH λ (microns)

Fig. 4.

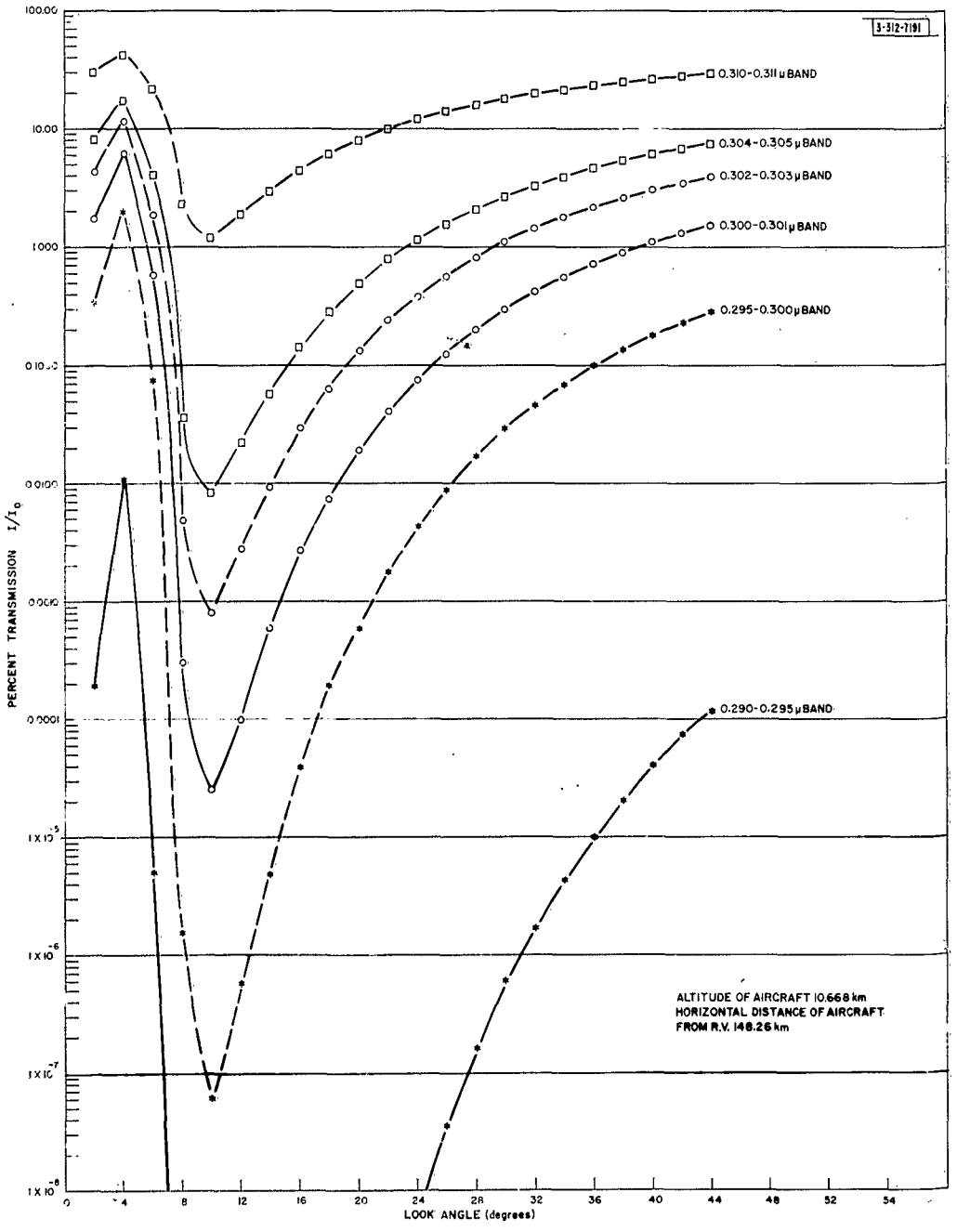
3-312-7191
0.310-0.311 μ BAND
0.304-0.305 μ BAND
0.302-0.303 μ BAND
0.300-0.301 μ BAND
0.295-0.300 μ BAND
0.290-0.295 μ BAND
ALTITUDE OF AIRCRAFT 10.668 km
HORIZONTAL DISTANCE OF AIRCRAFT FROM R.V. 148.26 km
PERCENT TRANSMISSION I/I_0
LOOK ANGLE (degrees)
100.00
10.00
1.000
0.0100
0.0001
1 X 10⁻⁵
1 X 10⁻⁶
1 X 10⁻⁷
1 X 10⁻⁸
0
4
8
12
16
20
24
28
32
36
40
44
48
52
54

Fig. 5.

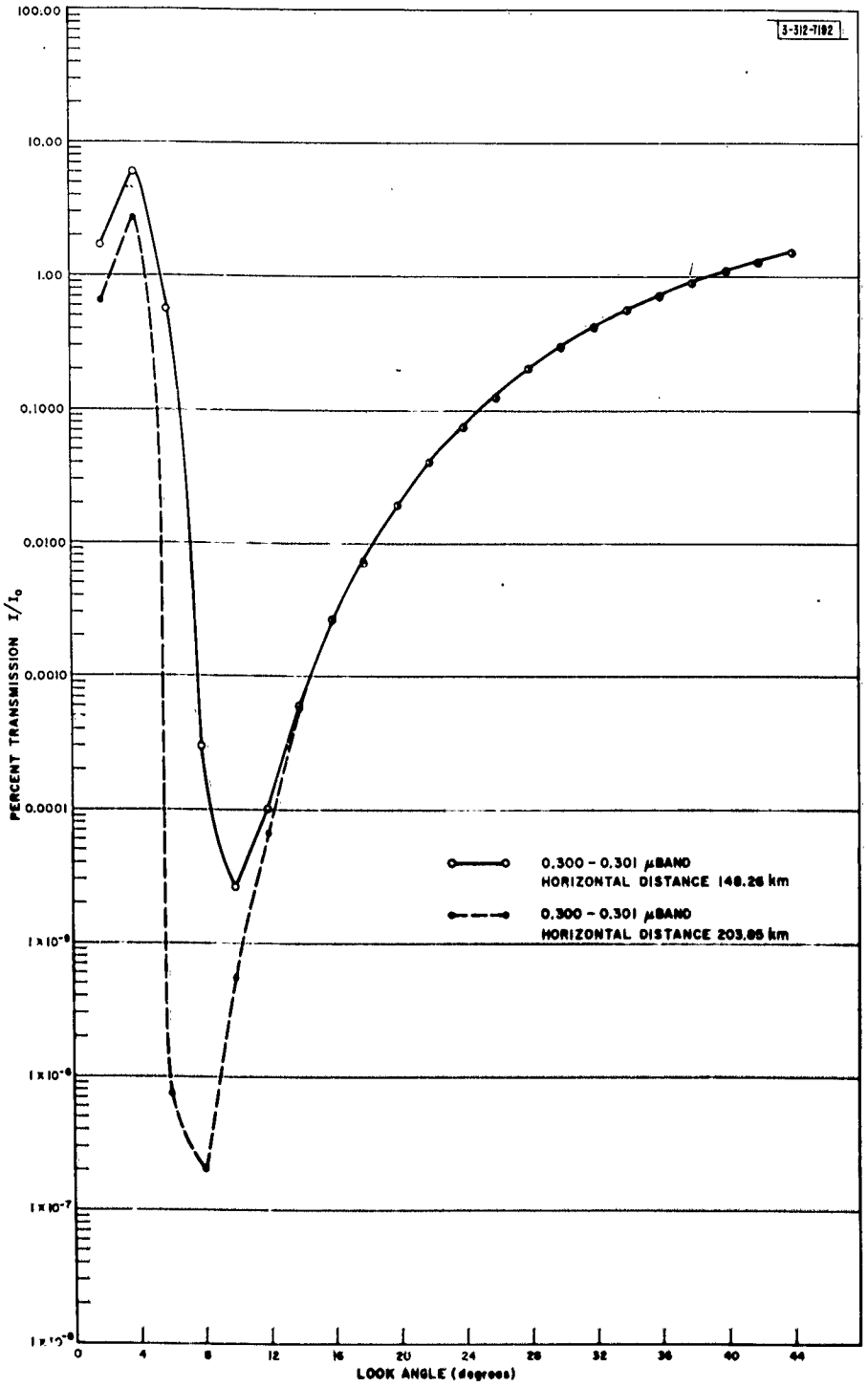
3-312-7192
100.00
10.00
1.00
0.1000
0.0100
0.0010
0.0001
PERCENT TRANSMISSION I/I₀
0.300 - 0.301 μBAND
HORIZONTAL DISTANCE 148.26 km
0.300 - 0.301 μBAND
HORIZONTAL DISTANCE 203.85 km
0
4
8
12
16
20
24
28
32
36
40
44
LOOK ANGLE (degrees)

Fig. 6.